J. Plasma Physics (2006), *vol.* 72, *part* 2, *pp.* 213–228. © 2005 Cambridge University Press
doi:10.1017/S0022377805003880 First published online 25 November 2005 Printed in the United Kingdom

Axisymmetric equilibria with anisotropic resistivity and toroidal flow

G. POULIPOULIS[1], G.N. THROUMOULOPOULOS[1] and H. TASSO[2]

[1]University of Ioannina, Association Euratom, Hellenic Republic, Section of Theoretical Physics, GR 451 10 Ioannina, Greece

[2]Max-Planck-Institut für Plasmaphysik, Euratom Association, D-85748 Garching, Germany
(gthroum@cc.uoi.gr)

(Received 10 February 2005 and accepted 1 March 2005)

Abstract. The equilibrium of an axisymmetric magnetically confined plasma with anisotropic resistivity and toroidal flow is investigated within the framework of magnetohydrodynamics (MHD). The stationary states are determined by an elliptic differential equation for the poloidal magnetic flux function ψ, a Bernoulli equation for the pressure and two relations for the resistivity components $\eta_\parallel$ and $\eta_\perp$ parallel and perpendicular to the magnetic field, respectively. The flow can affect the equilibrium properties solely in the presence of toroidicity because in the limit of infinite aspect ratio, the axial velocity does not appear in the equilibrium equations. The equilibrium characteristics of a tokamak with rectangular cross-section are studied by means of eigenfunctions in connection with exact solutions for the cases of 'compressible' flows with constant temperature, $T(\psi)$, but varying density on magnetic surfaces and incompressible ones with constant density, $\varrho(\psi)$, but varying temperature thereon. Those eigenfunctions can describe either single or multiple toroidal configurations. In the former case the equilibrium has the following characteristics: (i) the $\eta_\parallel$- and $\eta_\perp$-profiles on the poloidal cross-section having a minimum close to the magnetic axis, taking large values on the boundary and satisfying the relation $\eta_\perp > \eta_\parallel$ are roughly collisional; (ii) the electric field perpendicular to the magnetic surfaces possesses two local extrema within the plasma and vanishes on the boundary; and (iii) the toroidal current density is peaked close to the magnetic axis and vanishes on the boundary. The impact of the flow and the aspect ratio on the aforementioned quantities is evaluated for both 'compressible' and incompressible flows.

1. Introduction

Understanding the equilibrium properties of a magnetically confined plasma is one of the key issues in fusion research. The majority of equilibrium studies up to date concern plasmas of zero electrical resistivity and have been based on the Grad–Schlüter–Shafranov equation which describes the magnetohydrodynamic (MHD) equilibria of axisymmetric plasmas. Additional physical input in terms of resistivity and plasma flow, however, are very important. In addition to its apparent role for Ohmic heating, the importance of resistivity is connected to the operation of a

https://doi.org/10.1017/S0022377805003880 Published online by Cambridge University Press

steady-state fusion reactor which will involve time scales much longer than the resistive MHD one. Also an attractive feature of such a reactor would be operation under minimum sources of mass, momentum and energy. Sheared flow plays a key role in the formation of both edge transport barriers (L–H transition) [1, 2] and internal transport barriers [3–6] in tokamaks. This flow is associated with sheared electric field profiles [7–10] with significant amplitudes in the barrier region. Another pertinent quantity is the safety factor [11–13] which is closely related to the toroidal current density.

Theoretically it was proved a long time ago [14] that axisymmetric resistive MHD equilibria with scalar resistivity uniform on magnetic surfaces are not compatible with the Grad–Schlüter–Shafranov equation and the poloidal current density should vanish. The non-existence of axisymmetric equilibria with constant resistivity was also suggested in [15, 16]. To examine whether these undesirable properties can be removed by including, in addition to resistivity in Ohm's law, flow and viscosity terms in the momentum equation is a formidable task, which should be preceded by a step by step thorough investigation of particular cases, possibly introducing additional physical input each time. In this respect two of the authors of the present paper studied axisymmetric equilibria with scalar resistivity and purely toroidal flow [17] and flow parallel to the magnetic field $\mathbf{B}$ [18], and found that the flows considered cannot remove the aforementioned inconsistencies. Non-vanishing poloidal currents are possible in steady states with parallel flows in the presence of anisotropy, i.e. for different resistivity components $\eta_\parallel$ and $\eta_\perp$ parallel and perpendicular to $\mathbf{B}$ [19]; however, in this case neither $\eta_\parallel$ nor $\eta_\perp$ can be uniform on magnetic surfaces. The sole external source in [17–19] is the toroidal current loop voltage. Resistive equilibria, in a similar spirit of minimum external sources, were investigated in [15, 16, 20–24]. The particular flow directions considered in [17–19] are not inconsistent with Pfirsch–Schlüter diffusion in the sense that the equilibrium solutions constructed therein neither exclude nor can be included in possible Pfirsch–Schlüter diffusion solutions (having velocity components perpendicular to the magnetic surfaces). Also, we remind the reader that the pertinent pioneering study [25] does not include external sources of current and neglects the flow term in the momentum equation.

In this paper we extend the studies of [17–19] to equilibria with toroidal flows and anisotropic resistivity. There are two advantageous features of toroidal flows compared with parallel ones: (i) they are associated with electric fields $\mathbf{E}_\mathrm{p}$ perpendicular to the magnetic surfaces and (ii) as we will show exact solutions with magnetic surfaces of uniform temperature, $T = T(\psi)$, are possible. Equilibria with incompressible flows having uniform density but varying temperature on magnetic surfaces will also be examined. In this respect it is noted that although purely toroidal axisymmetric flows are inherently incompressible because of symmetry, $T(\psi)$ equilibria can be regarded as 'compressible' in the sense that the density varies on magnetic surfaces. In both cases the study can be carried out analytically up to the construction of exact solutions. In particular, equilibrium eigenstates of a tokamak with rectangular cross-section will be derived in connection with exact solutions describing either single toroidal or multitoroidal configurations. Furthermore, for single toroidal eigenstates we will study the characteristics of the conductivity components $\sigma_\parallel$ and $\sigma_\perp$, the electric field $\mathbf{E}_\mathrm{p}$, and the toroidal current density J_ϕ along with the impact of the flow on these quantities. This impact will be examined by varying a sound-speed Mach number M_0 for 'compressible' flows and

https://doi.org/10.1017/S0022377805003880 Published online by Cambridge University Press

a parameter A relating to the ϱ and $\mathbf{E}_{\mathrm{p}}$ profiles, and their variation perpendicular to the magnetic surfaces for incompressible ones. In particular, the uniformity of $\sigma_{\parallel}$ and $\sigma_{\perp}$ on magnetic surfaces will be examined independent of solutions. Also it will be shown that the impact of the flow on the equilibrium is crucially related to the toroidicity.

An outline of the paper is as follows. Reduced equilibrium equations involving ψ, the pressure and the resistivity components are derived in Section 2. Tokamak eigenstates are constructed in Section 3 for both 'compressible' and incompressible flows. The equilibrium characteristics of $\sigma_{\perp}$, $\sigma_{\parallel}$, $\mathbf{E}_{\mathrm{p}}$, and J_{ϕ} along with the impact of the flow and the aspect ratio on them is the subject of Section 4. The possible role of the flow shear is also briefly discussed therein. Conclusions are summarized in Section 5.

2. Equilibrium equations

In this section we shall derive reduced equilibrium equations for an axisymmetric magnetically confined plasma with anisotropic resistivity and toroidal flow. The procedure is unified in the sense that relevant energy equations or equations of state are not adopted from the beginning; they will specified when necessary later.

The starting equations in standard notation and convenient units are as follows:

$$\boldsymbol{\nabla}\cdot(\varrho\mathbf{v})=0, \tag{1}$$

$$\varrho(\mathbf{v}\cdot\boldsymbol{\nabla})\mathbf{v}=\mathbf{J}\times\mathbf{B}-\boldsymbol{\nabla}P, \tag{2}$$

$$\boldsymbol{\nabla}\times\mathbf{E}=0, \tag{3}$$

$$\boldsymbol{\nabla}\times\mathbf{B}=\mathbf{J}, \tag{4}$$

$$\boldsymbol{\nabla}\cdot\mathbf{B}=0, \tag{5}$$

$$\mathbf{E}+\mathbf{v}\times\mathbf{B}=\boldsymbol{\eta}\cdot\mathbf{J}=\eta_{\parallel}\cdot\mathbf{J}_{\parallel}+\eta_{\perp}\mathbf{J}_{\perp}, \tag{6}$$

$$\text{An energy equation or equation of state,} \tag{7}$$

where

$$\boldsymbol{\eta}=\begin{pmatrix}\eta_{\parallel} & 0\\ 0 & \eta_{\perp}\end{pmatrix} \tag{8}$$

is the resistivity tensor; the indices $\parallel$ and $\perp$ indicate directions parallel and perpendicular to $\mathbf{B}$; accordingly $\mathbf{J}_{\parallel}=(\mathbf{J}\cdot\mathbf{b})\mathbf{b}$, $\mathbf{J}_{\perp}=\mathbf{b}\times(\mathbf{J}\times\mathbf{b})=\mathbf{J}-\mathbf{J}_{\parallel}$, with $\mathbf{b}=\mathbf{B}/B$. The procedure to follow is based on identifying some integrals as flux functions, i.e. functions constant on magnetic surfaces, and reducing the set of equations (1)–(6) by projecting the momentum equation (2) and Ohm's law (6) along the toroidal direction, the poloidal one (or parallel to $\mathbf{B}$ when convenient) and perpendicular to the magnetic surfaces. Important information is also drawn from an integral form of (6) (see (13) below).

In cylindrical coordinates (R,ϕ,z), with z corresponding to the axis of symmetry, the equilibrium quantities for the case under consideration do not depend on the toroidal angle ϕ. The toroidal velocity and the divergence-free magnetic field and current density can be expressed, with the aid of Ampère's law, in terms of the

https://doi.org/10.1017/S0022377805003880 Published online by Cambridge University Press

functions $K(R,z)$, $\psi(R,z)$ and $I(R,z)$ as

$$\varrho\mathbf{v} = K\nabla\phi, \tag{9}$$

$$\mathbf{B} = I\nabla\phi + \nabla\phi\times\nabla\psi, \tag{10}$$

$$\mathbf{J} = \Delta^*\psi\nabla\phi - \nabla\phi\times\nabla I, \tag{11}$$

where ψ labels the magnetic surfaces and $\Delta^* \equiv R^2\nabla\cdot(\nabla/R^2)$.

By projecting the momentum equation along the toroidal direction one obtains

$$\nabla\phi\cdot(\nabla\psi\times\nabla I) = 0, \tag{12}$$

which implies that $I = I(\psi)$. Therefore, unlike the case of parallel flow [19], the current surfaces coincide with the magnetic ones irrespective of the equation of state. Integration of (6) along a contour c defined by the cut of an arbitrary current surface with the poloidal plane yields the equation

$$\int_c \mathbf{E}\cdot d\mathbf{l} + \int_c (\mathbf{v}\times\mathbf{B})\cdot d\mathbf{l} = \int_c (\boldsymbol{\eta}\cdot\mathbf{J})\cdot d\mathbf{l}, \tag{13}$$

where $d\mathbf{l} = \nabla\phi\times\nabla\psi/|\nabla\phi\times\nabla\psi|$ is the unit vector along the poloidal direction. Since in equilibrium it holds that $\partial\mathbf{B}/\partial t = 0$, the first integral on the left-hand side of (13) vanishes by Stoke's theorem. Also the second integral vanishes due to the toroidal direction of the flow. For the integral on the right-hand side to vanish the integrand must necessarily do so because the $\mathbf{J}_{\rm pol}$ lines are closed, nested and $\nabla\cdot\mathbf{J} = 0$; therefore it should hold locally that

$$(\boldsymbol{\eta}\cdot\mathbf{J})\cdot d\mathbf{l} = (\boldsymbol{\eta}\cdot\mathbf{J})_{\rm pol} = 0. \tag{14}$$

For isotropic resistivity, $\eta_\perp = \eta_\parallel$, (14) implies that the poloidal current density must vanish. In the presence of anisotropy, however, non-vanishing poloidal current densities are possible (as expected) because the toroidal electric field can drive a current in the poloidal direction. The rest of the report concerns equilibria with non-vanishing poloidal current densities.

Expressing the electric field on the poloidal cross-section in terms of the electrostatic potential, $\mathbf{E}_{\rm p} = -\nabla\Phi$, the component of the local Ohm's law (6) in the poloidal direction on account of (14) yields

$$\nabla\phi\cdot(\nabla\Phi\times\nabla\psi) = 0. \tag{15}$$

This implies that $\Phi = \Phi(\psi)$; therefore $\mathbf{E}_{\rm p}$ is perpendicular to the magnetic surfaces. The total electric field is given by

$$\mathbf{E} = V_{\rm c}\nabla\phi + \mathbf{E}_{\rm p} = V_{\rm c}\nabla\phi - \Phi'\nabla\psi,$$

where $2\pi V_{\rm c}$ is the constant toroidal loop voltage and the prime denotes a derivative with respect to ψ. Subsequently, the component of (6) along $\nabla\psi$ yields

$$\left(\Phi' - \frac{K}{\varrho R^2}\right)|\nabla\psi|^2 = 0, \tag{16}$$

and therefore the quantity

$$\frac{K}{\varrho R^2} \equiv \omega = \Phi', \tag{17}$$

identified as the rotation frequency, is a flux function $\omega = \omega(\psi)$. Equation (14) and the component of (6) in the toroidal direction, respectively, yield the following

https://doi.org/10.1017/S0022377805003880 Published online by Cambridge University Press

equations:

$$-\frac{\Delta\eta}{(BR)^2}(I\Delta^*\psi - I'|\nabla\psi|^2) - \eta_\perp I' = 0, \tag{18}$$

$$V_c = \Delta\eta\frac{I}{(BR)^2}[I'|\nabla\psi|^2 - I\Delta^*\psi] + \eta_\perp\Delta^*\psi, \tag{19}$$

where $\Delta\eta = \eta_\perp - \eta_\parallel$. Any equilibrium solution should be compatible with (18) and (19) which, accordingly, can be solved for $\eta_\perp$ and $\eta_\parallel$ to yield

$$\eta_\perp = \frac{V_c}{\Delta^*\psi + II'}, \tag{20}$$

$$\eta_\parallel = \eta_\perp\left(1 + \frac{I'(BR)^2}{I\Delta^*\psi - I'|\nabla\psi|^2}\right). \tag{21}$$

With the aid of the integrals $I = I(\psi)$, $\Phi = \Phi(\psi)$ and $\omega = \omega(\psi)$, the components of (2) along $\mathbf{B}$ and $\nabla\psi$, respectively, yield

$$\left[\frac{\nabla P}{\varrho} - \nabla\left(\frac{\omega^2R^2}{2}\right)\right]\cdot\mathbf{B} = 0, \tag{22}$$

$$[\Delta^*\psi + II']|\nabla\psi|^2 + R^2\left[\nabla P - \varrho\omega^2\nabla\left(\frac{R^2}{2}\right)\right]\cdot\nabla\psi = 0. \tag{23}$$

Owing to the axisymmetry and the toroidal direction of the flow these equations do not contain the resistivity and are identical in form to the respective ideal MHD equations.

In order to reduce (22) and (23) further an energy equation or equation of state is necessary. Owing to the large heat conduction along $\mathbf{B}$, isothermal magnetic surfaces, $T = T(\psi)$ is an appropriate equation of state for fusion plasmas. In this case employing the ideal gas law, $P = \lambda\varrho T$, integration of (22) yields

$$P = P_s(\psi)\exp\left(\frac{\omega^2R^2}{2\lambda T}\right) \tag{24}$$

where $P_s(\psi)$ is the pressure in the absence of flow. With the aid of (24), equation (23) leads to the final 'compressible' equation

$$\Delta^*\psi + II' + R^2\left[P_s' + P_s\frac{R^2}{2}\left(\frac{\omega^2}{\lambda T}\right)'\right]\exp\left(\frac{\omega^2R^2}{2\lambda T}\right) = 0. \tag{25}$$

For ideal plasmas ($\boldsymbol{\eta} = 0$) (25) was originally obtained in [26].

An alternative equation of state is incompressibility:

$$\nabla\cdot\mathbf{v} = 0. \tag{26}$$

Consequently, (1) implies that the density is a flux function, $\varrho = \varrho(\psi)$, and therefore along the same lines one can find the following incompressible equations for P and ψ:

$$P = P_s(\psi) + \frac{R^2\varrho\omega^2}{2} \tag{27}$$

$$\Delta^*\psi + II' + R^2P_s' + \frac{R^4}{2}(\varrho\omega^2)' = 0. \tag{28}$$

https://doi.org/10.1017/S0022377805003880 Published online by Cambridge University Press

Equation (28) is identical to a particular form of the axisymmetric equilibrium equation for incompressible flow in an arbitrary direction obtained in [27] for ideal plasmas.

Once (25) and (28) are solved for ψ, the resistivity components can be determined using (20) and (21). In general, inspection of (20) and (21) implies, as the case of parallel flows [19], that neither $\eta_\perp$ nor $\eta_\parallel$ can be uniform on magnetic surfaces; indeed solving (25) and (28) for $\Delta^\star\psi$ and substituting into (20) and (21), one can see that $\eta_\perp$ and $\eta_\parallel$ depend, in addition to ψ, explicitly on R (and on $|\nabla\psi|^2$ concerning $\eta_\parallel$). However, as we will see in Section 4, $\eta_\perp$ and $\eta_\parallel$ can be collisional-like, namely they can have a minimum close to the magnetic axis, take very large values on the boundary and it holds that $\eta_\perp > \eta_\parallel$. Reasons for temperature deviations on magnetic surfaces, which can result in non-uniformity of $\eta_\parallel$ and $\eta_\perp$ thereon, are discussed in Sec. III of [19].

Summarizing this section, the MHD equilibrium states of an axisymmetric plasma with anisotropic resistivity and toroidal flow are governed by an elliptic differential equation for the poloidal magnetic flux function (see (25) for 'compressible' flow and (28) for incompressible flow), a Bernoulli relation for the pressure and self-consistent expressions for the resistivities $\eta_\parallel$ and $\eta_\perp$. Both (25) and (28) contain four flux functions, three out of which, i.e. P_s, I and ω, are common. The fourth function is T for the 'compressible' equation and ϱ for the incompressible one. For vanishing flow (25) and (28) reduce to the Grad–Schlüter–Shafranov equation.

3. Exact solutions

Linearized forms of (25) and (28) in connection with appropriate assignments of the free flux functions they contain can be solved analytically. In the present study we will employ exact solutions as follows.

'Compressible' flow

The ansatz used to linearize (25) is [28, 29]

$$\begin{aligned} I^2 &= I_0^2 + I_1^2\psi^2 \\ P_s &= 2P_0\psi^2 \\ \frac{\omega^2}{\lambda T} &= \frac{\gamma M_0^2}{R_0^2} = \text{constant}. \end{aligned} \tag{29}$$

Here, I_0/R is the toroidal vacuum field, the parameter I_1 describes the magnetic properties of the plasma; P_0, γ and M_0 are a pressure parameter, the ratio of specific heats and the Mach number with respect to the speed of sound at a reference point ($z = 0, R = R_0$) with R_0 to be specified later. Note that the toroidal current density profile can vanish on the plasma boundary via (10).

Equation (25) then has a separable solution, $\mathscr{R}(R)\mathscr{Z}(z)$, when the constant of separation is equal to $R_0 I_1$. For configurations symmetric with respect to the mid-plane $z = 0$, this solution is written in the form

$$\psi(x,y) = C_1\left[J_0\left(\frac{2\tau\sqrt{e^{\gamma M_0^2 x^2/2}}}{\gamma {M_0}^2}\right) + C_2 Y_0\left(\frac{2\tau\sqrt{e^{\gamma M_0^2 x^2/2}}}{\gamma {M_0}^2}\right)\right]\cos(R_0 I_1 y), \tag{30}$$

where $x = R/R_0$ and $y = z/R_0$; J_0 and Y_0 are zeroth-order Bessel functions of the first and second kinds, respectively, and $\tau^2 \equiv 4P_0 R_0^4$.

https://doi.org/10.1017/S0022377805003880 Published online by Cambridge University Press

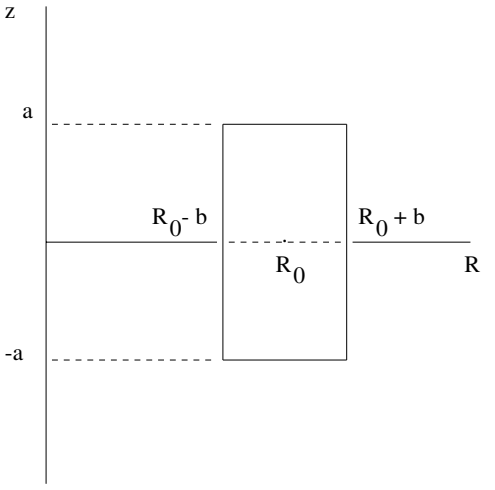


Figure 1. The cross-section of the plasma boundary. The aspect ratio α is defined as R_0/b, where R_0 is the geometric centre of the configuration.

Incompressible flow

In this case the ansatz employed to linearize (28) is [30]

$$\begin{aligned} I^2 &= I_0^2 + I_1^2\psi^2 \\ P_{\mathrm{s}} &= 2P_0\psi^2 \\ (\varrho\omega^2)' &= \left(\frac{K^2}{\varrho R^4}\right)' = 2A\psi. \end{aligned} \tag{31}$$

The third equation of (31) (on account of (17)) indicates that A is associated with the density and electric field profiles and their variation (shear) perpendicular to the magnetic surfaces ($(\varrho\omega^2)' \neq 0$). The polarity of $\mathbf{E}_{\mathrm{p}}$ and the aforementioned shear permits A to take either positive or negative values. This is a remarkable difference compared with the choice (29) which is shearless ($(\omega^2/\lambda T)' = 0$). Also, note that, unlike M_0 in (29), A is dimensional.

A separable solution is now expressed in terms of Airy functions of the first and second kinds, Ai and Bi, as [30]

$$\begin{aligned} \psi(x,y) = C_1 \Bigg[& Ai\left(\left(\frac{AR_0}{4}\right)^{-2/3}\left(\frac{AR_0^6}{4}x^2 - P_1R_0^4\right)\right) \\ & + C_2 Bi\left(\left(\frac{AR_0}{4}\right)^{-2/3}\left(\frac{AR_0^6}{4}x^2 - P_1R_0^4\right)\right)\Bigg] \cos\left(R_0 I_1 y\right). \end{aligned} \tag{32}$$

In connection with solutions (30) and (32) we are interested in the steady states of a tokamak for which the plasma is bounded by a conducting wall of rectangular cross-section, as shown in Fig. 1. In addition, we assume that the plasma boundary coincides with the outermost magnetic surface. Thus, the magnetic field is tangential to the boundary and the pressure P must vanish on the boundary†;

† The consequences of the toroidal electric field on the boundary conditions are discussed in more detail in [17, 18].

https://doi.org/10.1017/S0022377805003880 Published online by Cambridge University Press

accordingly, the function ψ should satisfy the following boundary conditions:

$$\psi(y_\pm) = 0 \tag{33}$$

and

$$\psi(x_\pm) = 0, \tag{34}$$

where $y_\pm = \pm a/R_0$ and $x_\pm = 1 \pm b/R_0$. The equilibrium then becomes a boundary-value problem. Eigenstates can be determined by imposing conditions (33) and (34) directly to the solutions (30) and (32). Specifically, (33) applied to the z-dependent part of the solutions yields the eigenvalues

$$I_1^\ell = \frac{1}{a}\left(\ell\pi - \frac{\pi}{2}\right), \quad \ell = 1, 2, \dots \tag{35}$$

for the quantity I_1, which is related to the poloidal current function $I(\psi)$. The respective eigenfunctions are associated with configurations possessing ℓ magnetic axes parallel to the axis of symmetry. Condition (34) is pertinent to the R-dependent part of the solution. Owing to the flow this part contains the parameter M_0 in the 'compressible' case and A in the incompressible case, in addition to the pressure parameter P_0. Thus, condition (34) can determine flow eigenvalues depending on the parameter P_0 which remains free, $F^n(P_0)$ $(n = 1, 2, 3, \dots)$ with F standing for either M_0 or A, or *vice versa*, pressure eigenvalues $P_0^n(F)$ with F being free. The other parameters C_1 and C_2 contained in (30) and (32) are adapted to normalize ψ with respect to the magnetic axis and to satisfy the boundary condition (34), respectively. The eigenfunctions in association with $F^n(P_0)$ (or $P_0^n(F)$) are connected to configurations having n magnetic axes perpendicular to the axis of symmetry. Therefore the total equilibrium eigenfunctions $\psi_{\ell n} = \mathscr{Z}_\ell(z)\mathscr{R}_n(R)$ describe multitoroidal configurations having $\ell \times n$ magnetic axes.

On the basis of the above solutions one can evaluate the impact of the flow on the resistivity components $\eta_\perp$ (20) and $\eta_\parallel$ (21), the electric field perpendicular to the magnetic surfaces ($\mathbf{E}_\mathrm{p} = -\nabla\Phi = -\Phi'\nabla\psi$) and the toroidal current density J_ϕ (11) for both 'compressible' and incompressible flows. It is emphasized that this impact is crucially related to the toroidicity because in the limit of infinite aspect ratio, the equilibrium equations do not contain the axial velocity regardless of 'compressibility'. Indeed, for a cylindrical plasma of arbitrary cross-section the equations corresponding to (22) and (23) read as

$$\mathbf{B} \cdot \nabla P = 0 \tag{36}$$

$$\nabla^2\psi + \left(P + \frac{B_z^2}{2}\right)' = 0. \tag{37}$$

For ideal plasmas (36) and (37) follow, respectively, from (16) and (17) of [31] for vanishing poloidal velocity ($F' = 0$ therein). Therefore the flow may have an impact on equilibrium only in the presence of toroidicity. Also, note that the pressure becomes a flux function. Because of the importance of toroidicity, the impact of the aspect ratio on equilibrium in addition to that of the flow will be evaluated in the next section.

https://doi.org/10.1017/S0022377805003880 Published online by Cambridge University Press

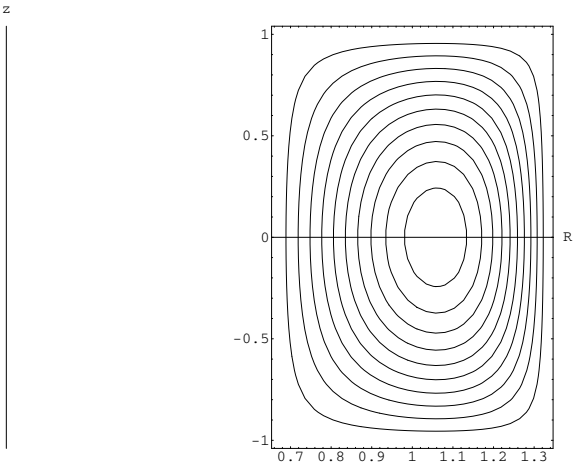


Figure 2. Magnetic surface cross-sections for the single toroidal configuration in connection with the eigenfunction ψ_{11} for $M_0 = 0.5$ and $\alpha = 3$.

4. Impact of the flow and aspect ratio on equilibrium

The quantities to be examined are the conductivity components $\sigma_\perp = 1/\eta_\perp$ and $\sigma_\parallel = 1/\eta_\parallel$, the electric field $\mathbf{E}_\mathrm{p}$ and the toroidal current density J_ϕ. Both 'compressible' and incompressible flows will be studied for single toroidal configurations. The study is based on the eigenfunction ψ_{11} which for a 'compressible' flow is shown in Fig. 2 and will be made by varying the flow parameters M_0 and A for 'compressible' and incompressible flows, respectively. For any value of M_0 or A, the respective lowest eigenvalue of the pressure parameter P_0 will be calculated numerically. The variation of M_0 and A will correspond to the same range of eigenvalues of P_0. Specifically, for aspect ratio $\alpha = 3$ the flow parameters M_0 and A will be ranged in the intervals $[0.1, 0.7]$ and $[-0.001, -0.01]$, respectively. For $\alpha = 2$ the respective intervals will be $[0.1, 1]$ and $[-0.001, -0.08]$ unless stated otherwise. Variation of the flow parameters in connection with the results to be presented will refer to these intervals. The tokamak scaling $B_\mathrm{p} \approx 0.1 B_\phi$ will be used for the calculations. Also, we should make the following clarification: solutions (30) and (32) oscillate as the flow parameters are varied, namely for any given point (R, z) these solutions considered as functions $\psi(M_0)$ and $\psi(A)$ take successively larger and lower values as M_0 and A are varied monotonically. This would give rise to an oscillatory behaviour to all physical quantities which is physically unjustifiable. For the conductivity components this can be seen in Fig. 3. To avoid this difficulty the solutions will be normalized in such a way that the poloidal magnetic flux on the magnetic axis is unity irrespective of flow. This is accomplished by choosing the parameter C_1 appropriately for each value of M_0 or A ($C_1(M_0)$ for 'compressible' flow and $C_1(A)$ for incompressible flow). Also, solutions (30) and (32) have a strong parametric dependence on the flow parameters (note the exponential dependence of (30) on M_0^2). Consequently, this dependence results in large quantitative changes in the physical quantities for large M_0 ($M_0 \approx 1$) or small A ($A \approx -0.01$) which most probably overestimate the impact of flow. In addition, it is noted that except for the conductivity components, an increase of M_0 has qualitatively the same impact on the physical quantities to be examined as that caused by a decrease of A.

https://doi.org/10.1017/S0022377805003880 Published online by Cambridge University Press

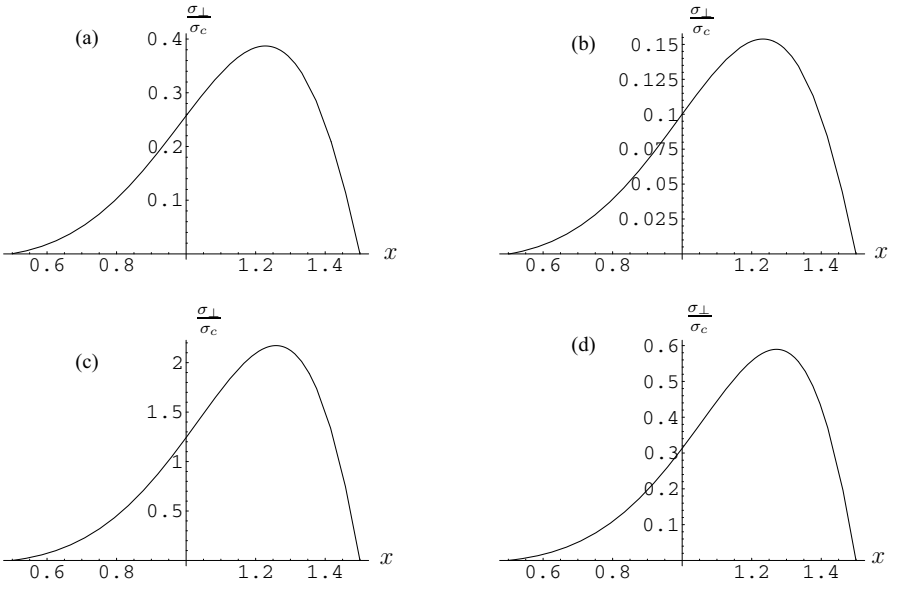


Figure 3. A set of curves demonstrating the oscillation of the profile of $\sigma_\perp$ on the mid-plane $z = 0$, normalized with respect to a constant value σ_c, for 'compressible' flow when the value of the function ψ on the magnetic axis is flow-dependent and the Mach number M_0 increases: (a) $M_0 = 0.1$, (b) $M_0 = 0.2$, (c) $M_0 = 0.5$ and (d) $M_0 = 0.6$. The aspect ratio is $\alpha = 2$; $x \equiv R/R_0$ with the vertical axis being placed at the position of the geometric centre ($x = 1$).

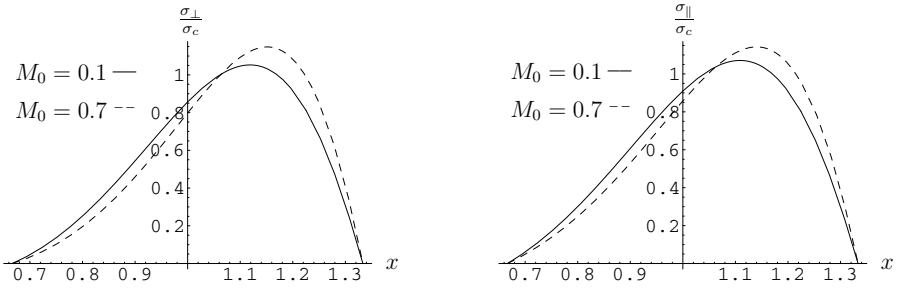


Figure 4. The figure shows the increase of the maximum of $\sigma_\perp$ and $\sigma_\parallel$ and the displacement of its position outwards for 'compressible' flow due to the increase of the Mach number M_0.

The results concerning the characteristics of the quantities $\sigma_\perp$, $\sigma_\parallel$, $\mathbf{E}_\mathrm{p}$ and J_ϕ and the impact of the flow and α on them are as follows.

Conductivity components

(1) For both 'compressible' and incompressible flows, the profiles of $\sigma_\perp$ and $\sigma_\parallel$ on the poloidal cross-section are collisional-like, i.e. they have a maximum close to the magnetic axis, vanish on the boundary and in most cases $\sigma_\parallel > \sigma_\perp$. Profiles of the resistivity components on the mid-plane $z = 0$ are shown in Fig. 4 for 'compressible' flows and in Fig. 5 for incompressible ones. For vanishing flow and $\alpha = 3$ one finds $\Delta\sigma/\sigma_\parallel \equiv (\sigma_\parallel - \sigma_\perp)/\sigma_\parallel = 0.2122$; for the reversed-field-pinch scaling, $B_\phi \approx B_\mathrm{p}$, the value of $(\sigma_\parallel - \sigma_\perp)/\sigma_\parallel$ doubles, i.e. 0.4244. Also, for $\alpha = 3$ an increase of M_0 from 0.1 to 0.7 results in a percentage decrease of $\Delta\sigma$ by 4% while a decrease of A from -0.001 to -0.01 leads to an increase of $\Delta\sigma$ by 3.4%.

https://doi.org/10.1017/S0022377805003880 Published online by Cambridge University Press

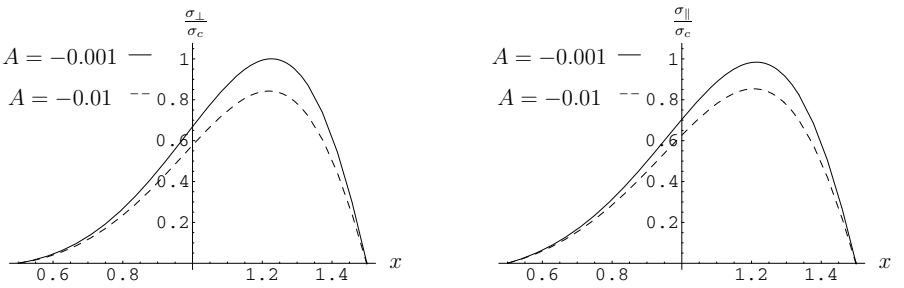


Figure 5. The figure shows the decrease of the maximum of $\sigma_\perp$ and $\sigma_\parallel$ but the insensitivity of its position for incompressible flow as the parameter A decreases.

(2) The maximum of the profiles takes larger values as M_0 increases and lower values as A decreases. For $\alpha = 3$ an increase of M_0 (from 0.1 to 0.7) leads to percentage increases of $\sigma_\perp$ and $\sigma_\parallel$ by 9% and 7%, respectively. For incompressible flows the respective decreases are 73% and 67% (for $\alpha = 3$ and a decrease of A from -0.001 to -0.01).

(3) The position of the maximum is shifted outwards from the axis of symmetry as M_0 increases and is nearly insensitive to the variation of A† (see Figs 4 and 5). For example, for $\alpha = 3$ the position of the maximum of $\sigma_\perp$ changes from 1.119 to 1.151 (when M_0 varies from 0.1 to 0.7).

(4) The lower α is:

- the larger the decrease of $\Delta\sigma = \sigma_\parallel - \sigma_\perp$ as M_0 increases;
- the smaller the increase of $\Delta\sigma$ as A decreases;
- the larger the increase of the $\sigma_\perp$ and $\sigma_\parallel$ maximum as M_0 increases;
- the smaller the decrease of the $\sigma_\perp$ and $\sigma_\parallel$ maximum as A decreases; and
- the larger the shift of the position of $\sigma_\perp$ and $\sigma_\parallel$ maximum as M_0 increases.

These conclusions become evident if the following results for $\alpha = 2$ are compared with those presented above for $\alpha = 3$:

- the decrease of $\Delta\sigma$ for compressible flow is 13%;
- the increase of $\Delta\sigma$ for incompressible flow is 1%. The respective variation of A in this case is $[-0.001, -0.01]$‡;
- the increase of the conductivity maximum values for 'compressible' flows is 44% ($\sigma_\perp$) and 27% ($\sigma_\parallel$);
- the decrease of the conductivity maximum values for incompressible flows is 43.7% ($\sigma_\perp$) and 63% ($\sigma_\parallel$); and
- the position of the maximum of $\sigma_\perp$ for a 'compressible' flow is displaced from 1.228 to 1.33.

† To be precise, for incompressible flow when A decreases the position of the maximum first is shifted outwards and then inwards when A take small negative values.

‡ For $\alpha = 2$ and very small algebraic values of A, i.e. $A \leqslant -0.08$, it holds that $\sigma_\parallel < \sigma_\perp$.

https://doi.org/10.1017/S0022377805003880 Published online by Cambridge University Press

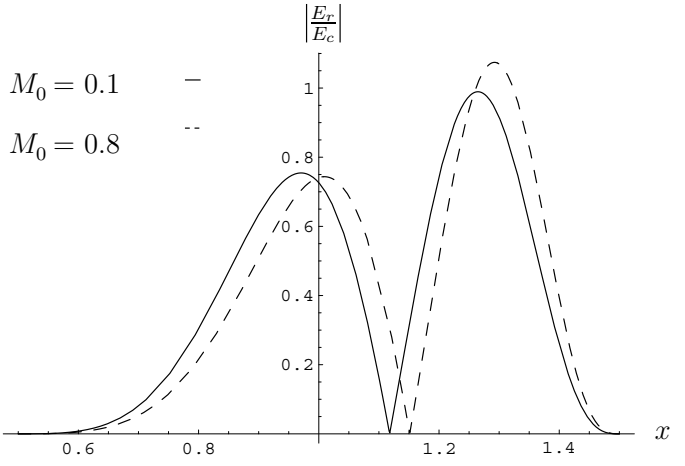


Figure 6. Electric field profiles on the mid-plane $z = 0$ for 'compressible' flow. A comparison of the two curves indicates the increase of the local maxima of $|\mathbf{E}_\mathrm{p}|$ and the outward shift of their positions as the Mach number M_0 increases from 0.8 to 1. The point in between the two maxima at which $\mathbf{E}_\mathrm{p} = 0$ corresponds to the magnetic axis. The aspect ratio is $\alpha = 2$ and the value of the shaping parameter n (see (38)) is 3.

The 'compressibility'-dependent impact of the flow on $\sigma_\perp$, $\sigma_\parallel$ and $\Delta\sigma$ may relate to the flow shear of the incompressible solution (32), while the 'compressible' solution (30) is shearless.

Electric field

Prescribing the rotation frequency $\omega(\psi)$ by

$$\omega = \omega_0 \psi^n, \tag{38}$$

where n is a shaping parameter, the electric field, $\mathbf{E}_\mathrm{p} = -\Phi'\nabla\psi$, with the help of (17) becomes

$$\mathbf{E}_\mathrm{p} = -\omega_0 \psi^n \nabla\psi. \tag{39}$$

The profile of $\mathbf{E}_\mathrm{p}$ on the poloidal cross-section possesses two local extrema within the plasma volume: one on the left-hand side and the other on the right-hand side of the magnetic axis with opposite sign, which means that the electric field has a different polarity (as can also be deduced from (39)) and is similar to those observed in equilibria with internal transport barriers. The profile $|E_r|$, on the mid-plane $y = 0$ is shown in Fig. 6. An increase of M_0 or a decrease of A leads to an increase of both local maximum values of $|E_r|$ with the outwards one being more than the one inwards with respect to the magnetic axis and to a displacement of their positions outwards. For 'compressible' flows this is shown in Fig. 6. For $\alpha = 3$ the maximum values of $|E_r|$ increase by 4% for 'compressible' flow (an increase of M_0 from 0.1 to 0.7) and 5.6% for incompressible flow (a decrease of A from -0.001 to -0.01). The lower α is, the larger the increase of the maxima and the displacement of their positions outwards. As an example, for $\alpha = 2$ the increase of the maximum $|E_r|$ becomes as large as 15% for 'compressible' flow with a strong increase occurring above $M_0 = 0.8$ and 9% for incompressible flow. Also, when the parameter n takes larger values, the maxima of $|E_r|$ take lower values but the profile of E_r becomes steeper and more localized (Fig. 7); therefore the shear $S_{E_r} = \partial E_r/\partial x$ is also increased.

https://doi.org/10.1017/S0022377805003880 Published online by Cambridge University Press

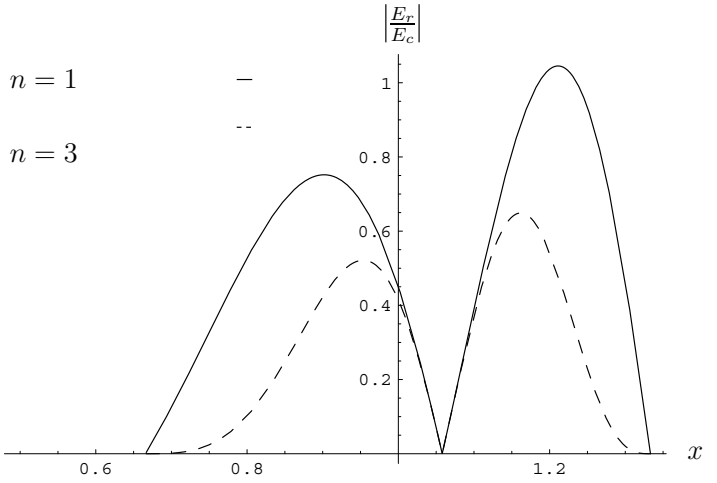


Figure 7. Electric field profiles on the mid-plane $z = 0$ for $\alpha = 3$, $M_0 = 0.4$ and two different values of the shaping parameter $n = 1$ and 3.

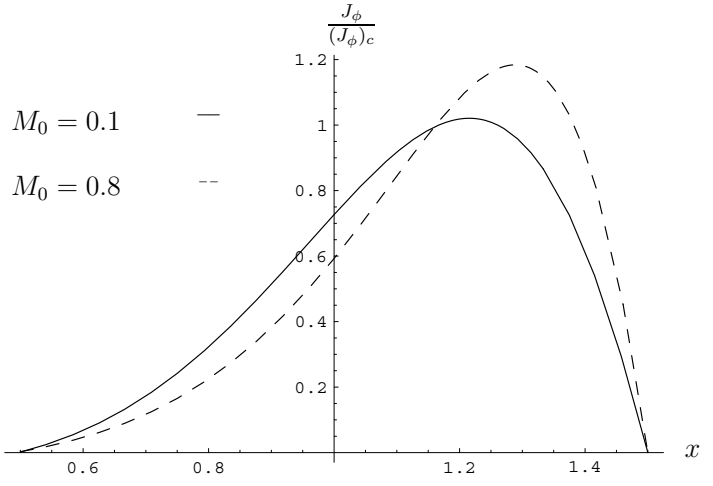


Figure 8. Toroidal current density profiles on the mid-plane $z = 0$ for 'compressible' flows. A comparison of the two curves indicates the increase of the maximum and the outward displacement of its position as the Mach number M_0 increases from 0.1 to 0.8. The aspect ratio is $\alpha = 2$.

The toroidal current density

The profile of the toroidal current density,

$$J_\phi = \frac{1}{R}\Delta^*\psi, \tag{40}$$

is peaked with its maximum in the vicinity of the magnetic axis and vanishes on the plasma boundary (Fig. 8). Like $\mathbf{E}_\mathrm{p}$, as M_0 increases or A decreases, the maximum of J_ϕ takes larger values and its position is displaced outwards. Also, the impact of the variation of the flow parameters is stronger as the aspect ratio becomes smaller. In particular, for $\alpha = 3$ and 2 the maximum value of the current density increases by 8

https://doi.org/10.1017/S0022377805003880 Published online by Cambridge University Press

and 35.5%, respectively, for 'compressible' flows (an increase of M_0). The respective increases for incompressible flows (a decrease of A) are 5.6 and 18%.

5. Conclusions

In this paper we have investigated the MHD equilibrium of an axisymmetric magnetically confined plasma with anisotropic resistivity and toroidal flow subjected to the single external source of a toroidal current loop voltage by including the flow term in the momentum equation. Equilibria of this kind are inherently free of Pfirsch–Schlüter diffusion. Also, unlike the case of parallel flows, there is an electric field $\mathbf{E}_\mathrm{p}$ perpendicular to the magnetic surfaces. The study includes 'compressible' flows with varying density but uniform temperature on magnetic surfaces and incompressible flows with uniform density but varying temperature thereon. It turns out that the equilibrium states are determined by an elliptic differential equation for the poloidal magnetic flux function ψ ((25) for 'compressible' flows and (28) for incompressible flows), a Bernoulli equation for the pressure (respectively (24) and (27)) and two relations for the resistivities $\eta_\perp$ (20) and $\eta_\parallel$ (21), parallel and perpendicular to the magnetic field. Owing to axisymmetry and the toroidal direction of the flow, the equilibrium equations and pressure relations are identical in form to the respective ideal MHD ones. The impact of the flow on equilibrium can be 'activated' solely in the presence of toroidicity because the cylindrical equilibrium equations do not contain the axial velocity.

The equilibrium of a tokamak plasma bounded by a rectangular cross-section has been studied by means of equilibrium eigenfunctions in connection with exact solutions for 'compressible' and incompressible flows. These eigenfunctions can describe either single toroidal or multiple toroidal configurations. In the former case we have studied the characteristics of the conductivities $\sigma_\perp$ and $\sigma_\parallel$, the electric field $\mathbf{E}_\mathrm{p}$ and the toroidal current density J_ϕ, as well as how they are affected by the flow. The impact of the flow has been examined by varying pertinent flow parameters, i.e. a sound-speed Mach number M_0 for the 'compressible' flow and a parameter A relating to the density and electric field and their variations perpendicular to the magnetic surfaces for the incompressible flow. For (i) single toroidal configurations, (ii) eigenfunctions normalized so that ψ is unity on the magnetic axis regardless of flow (a normalization made to avoid physically unjustifiable oscillation of the solutions on the flow parameters) and (iii) variation of the flow parameters corresponding to the same variation of the lowest eigenvalue for the pressure parameter P_0 we came to the following conclusions.

(1) For a toroidal frequency $\omega(\psi)$ peaked on the magnetic axis and vanishing on the boundary, (38), the profile of $|\mathbf{E}_\mathrm{p}|$ on the poloidal cross-section has two maxima, are located on the left-hand side and the other on the right-hand side of the magnetic axis, and it vanishes on the boundary. When the maximum of ω becomes larger and its profile more localized, the profile of $|\mathbf{E}_\mathrm{p}|$ also becomes more localized though its maxima become smaller.

(2) The profile of J_ϕ is peaked with its maximum close to the magnetic axis and vanishes on the boundary.

(3) Although the conductivity components cannot be uniform on magnetic surfaces (this follows in general by inspection of the equilibrium equations), their profiles

https://doi.org/10.1017/S0022377805003880 Published online by Cambridge University Press

are roughly collisional, namely they have a maximum in the vicinity of the magnetic axis, vanish on the boundary and, in most of the cases, it holds that $\sigma_\parallel > \sigma_\perp$.

(4) As M_0 increases or A decreases, the local maxima of $|\mathbf{E}_\mathrm{p}|$ and J_ϕ take larger values and their positions are shifted outwards from the axis of symmetry.

(5) The impact of the variation of the flow parameters on $\sigma_\perp$ and $\sigma_\parallel$ rely on 'compressibility': as for $|\mathbf{E}_\mathrm{p}|$ and J_ϕ, the maxima of $\sigma_\perp$ and $\sigma_\parallel$ become larger as M_0 increases and their positions are displaced outwards, but these maxima become smaller and their positions are nearly not affected as A decreases. Also, the larger the value of M_0 is, the smaller $\sigma_\parallel - \sigma_\perp$, but the smaller A is, the larger $\sigma_\parallel - \sigma_\perp$.

(6) For a given value of M_0, the lower the aspect ratio α is, the smaller the maxima of $\sigma_\parallel$, $\sigma_\perp$ and J_ϕ, but the larger the maxima of $|\mathbf{E}_\mathrm{p}|$.

(7) For a given value of A, the lower the aspect ratio α is, the larger the maxima of $\sigma_\parallel$, $\sigma_\perp$ and $|\mathbf{E}_\mathrm{p}|$, but the smaller the maximum of J_ϕ.

(8) For an increase of M_0 or a decrease of A (corresponding to the same variation of the lowest eigenvalue of P_0), the lower α is, the higher the variation of the maxima of $|\mathbf{E}_\mathrm{p}|$ and J_ϕ and the displacements of their positions outwards. The impact of α on the conductivities are 'compressibility'-dependent: the smaller the α is (i) the larger the variation of the maximum of $\sigma_\perp$, $\sigma_\parallel$ and $\sigma_\parallel - \sigma_\perp$ (when M_0 increases) but (ii) the smaller the maximum of $\sigma_\perp$, $\sigma_\parallel$ and $\sigma_\parallel - \sigma_\perp$ (when A decreases).

Qualitatively, except for the conductivity components, the impact of the flow on $\mathbf{E}_\mathrm{p}$ and J_ϕ is independent of 'compressibility'. The dependence of the results for $\sigma_\perp$ and $\sigma_\parallel$ on 'compressibility' may be due to the fact that the incompressible solution (32) has finite flow shear while the flow of the compressible one (30) is shearless. Quantitatively, for $\alpha = 2$ an increase of M_0 from 0.1 to 0.5 or a decrease of A from -0.001 to -0.006 results in percentage variations of all quantities ($\sigma_\parallel$, $\sigma_\perp$, $\mathbf{E}_\mathrm{p}$, and J_ϕ) of less that 10%. We have found larger variations of these quantities associated with higher values of M_0 or lower values of A, on the basis of solutions (30) and (32), most probably an overestimate of the actual impact of the flow.

Acknowledgement

Part of this work was conducted during a visit of the authors G.P. and G.N.T. to the Max-Planck-Institut für Plasmaphysik, Garching. The hospitality of that Institute is greatly appreciated.

References

[1] Terry, P. W. 2000 *Rev. Mod. Phys.* **72**, 109.
[2] deGrassie, J. S. et al. 2004 *Phys. Plasmas* **11**, 4323.
[3] Wang, A. K. et al. 2002 *Phys. Plasmas* **9**, 748.
[4] Fiore, C. L. et al. 2001 *Phys. Plasmas* **8**, 2023.
[5] Rice, J. E. et al. 2001 *Nucl. Fusion* **41**, 277.
[6] Connor, J. W. et al. 2001 *Nucl. Fusion* **44**, R1.

https://doi.org/10.1017/S0022377805003880 Published online by Cambridge University Press

[7] Burell, K. H. et al. 1994 *Phys. Plasmas* **1**, 1536.
[8] Mazzucato, E. et al. 1996 *Phys. Rev. Lett.* **77**, 3145.
[9] Bell, R. E. et al. 1998 *Phys. Rev. Lett.* **81**, 1429.
[10] Meister, H. et al. 2001 *Nucl. Fusion* **41**, 1633.
[11] Joffrin, E. et al. 2002 *Plasma Phys. Control. Fusion* **44**, 1739.
[12] Litaudon, X. et al. 1996 *Plasma Phys. Control. Fusion* **38**, 1603.
[13] Quigley, E. D. et al. 2004 *Nucl. Fusion* **44**, 1189.
[14] Tasso, H. 1979 *Lectures on Plasma Physics*, report IFUSP/P-181, LFP-8, Universidade de São Paulo, Instituto de Física, São Paulo (1979), p. 27. (See EPAPS Document No. E-PHPAEN-10-027306 for *Lectures on Plasma Physics*. A direct link to this document may be found in the online article's HTML reference section. The document may also be reached via the EPAPS homepage (http://www.aip.org/pubservs/epaps.html) or from ftp.aip.org in the directory /epaps/. See the EPAPS homepage for more information.)
[15] Montgomery, D. and Shan, X. 1994 *Comment Plasma Phys. Controlled Fusion* **15**, 315.
[16] Montgomery, D., Bates, J. W. and Lewis, H. R. 1997 *Phys. Plasmas* **4**, 1080.
[17] Throumoulopoulos, G. N. 1998 *J. Plasma Phys.* **59**, 303.
[18] Throumoulopoulos, G. N. and Tasso, H. 2000 *J. Plasma Phys.* **64**, 601.
[19] Throumoulopoulos, G. N. and Tasso, H. 2003 *Phys. Plasmas* **10**, 2382.
[20] Bates, J. W. and Lewis, H. R. 1996 *Phys. Plasmas* **3**, 2395.
[21] Goodman, M. L. 1998 *J. Plasma Phys.* **60**, 587.
[22] Bora, M. P. 2000 *Phys. Plasmas* **7**, 3097.
[23] Kamp, L. P. and Montgomery, D. 2003 *Phys. Plasmas* **10**, 157.
[24] Kamp, L. P. and Montgomery, D. 2004 *J. Plasma Phys.* **70**, 113.
[25] Pfirsch, D. and Schlüter, A. 1962 *Der Einfluß der elektrischen Leitfähigkeit auf das Gleichgewichtsverhalten von Plasmen niedringen Drucks in Stellaratoren*, Report MPI/PA/7/62, 1962, Max-Planck-Institut, Munich. (Also available as National Technical Information Document No. MPI/PA/7/62, Munich, 1962 by D. Pfirsch and A. Schlüter. Copies may be ordered from the National Technical Information Service, Springfield, VA 22161).
Wesson, J. 1997 *Tokamaks*, 2nd edn (*The Oxford Engineering Science Series*). New York: Oxford Science, p. 48.
[26] Maschke, E. K. and Perrin, H. 1980 *Plasma Phys.* **22**, 579.
[27] Tasso, H. and Throumoulopoulos, G. N. 1998 *Phys. Plasmas* **5**, 2378.
[28] Clemente, R. A. and Farengo, R. 1984 *Phys. Fluids* **27**, 776.
[29] Throumoulopoulos, G. N. and Pantis, G. 1989 *Phys. Fluids* B **1**, 1827.
[30] Throumoulopoulos, G. N., Poulipoulis, G., Pantis, G. and Tasso, H.. 2003 *Phys. Lett.* A **317**, 463.
[31] Throumoulopoulos, G. N. and Tasso, H. 1997 *Phys. Plasmas* **4**, 1492.

https://doi.org/10.1017/S0022377805003880 Published online by Cambridge University Press